International Journal of Mass Spectrometry 300 (2011) 2–11

Contents lists available at ScienceDirect

International Journal of Mass Spectrometry

journal homepage: www.elsevier.com/locate/ijms

# Electron ionization and gas-phase ion molecule reactions of methylcyclohexane

C.Q. Jiao [a], K.K. Irikura [b], S.F. Adams [c,*], A. Garscadden [d]

[a] UES, Inc., Dayton, OH 45432-1894, United States
[b] National Institute of Standards and Technology, Gaithersburg, MD 20899-8320, United States
[c] Air Force Research Laboratory, Wright-Patterson AFB, OH 45433-7251, United States
[d] Air Force Institute of Technology, Wright-Patterson AFB, OH 45433-7765, United States

ARTICLE INFO

*Article history:*
Received 8 September 2010
Received in revised form 28 October 2010
Accepted 1 November 2010
Available online 9 November 2010

*Keywords:*
Methylcyclohexane
Electron ionization
Ion molecule reaction
Cycloalkane
Binary-Encounter-Bethe model
Fourier-transform mass spectrometry

ABSTRACT

Absolute cross sections for electron ionization of methylcyclohexane (MCH, $C_7H_{14}$) are measured as a function of the electron energy in a range of 10–200 eV. The electron ionization of MCH produces the parent ion $C_7H_{14}^{+\bullet}$ and fragment ions $C_6H_{11}^+$ and $C_4H_7^+$ as the predominant product ions at most of the electron energies studied. Reactions between selected hydrocarbon ions with the neutral MCH molecule, mainly via hydride transfer, charge transfer and $H_2^-$ transfer mechanisms, are studied. Absolute rate constants are reported, and the correlations between the reactivities and the thermochemical data of the reactions are discussed. The Binary-Encounter-Bethe method is applied to MCH to provide a theoretical comparison to the sum of the measured ionization cross sections.



## 1. Introduction

Cycloalkanes are a significant component of many complex fuels. As examples, Jet-A fuel is composed of cycloalkanes up to 20% [1], and the JP-8 fuels are composed of mainly monocyclic and bicyclic alkanes [2]. Methylcyclohexane (MCH, $C_7H_{14}$) is one of the simpler cycloalkanes and has been chosen as the representative cycloalkane in surrogate mixtures for practical fuels [1,3–7]. Pyrolysis and oxidation of MCH in the vapor phase have been studied for the purpose of understanding the characteristics of the ignition and combustion of MCH [7–12]. The ion-molecule reactions involving MCH have been investigated in relation to the role played by ions in enhancing the combustion of hydrocarbon fuels [13], as the ion-molecule chemistry may be particularly advantageous to issues involving ignition and flame propagation [14]. In the investigation made by Midey et al. [13] the reactions of $O_2^+$, $NO^+$ and $H_3O^+$ with MCH were studied and found to be via the mechanisms of charge transfer, hydride transfer and proton transfer, respectively. It was found that the charge transfer and hydride transfer proceed at collision rates, while the proton transfer proceeds at a slower rate due to the involvement of significant rearrangement [13]. Other research groups have also studied the proton transfer reactions of MCH with $H_3O^+$ and other ions including $H_3^+$ and $N_2H^+$ [15,16]. In addition, the thermochemistry and kinetics of charge transfer between MCH and hydrocarbon ions have been measured [17].

In this paper the electron ionization cross sections of MCH, measured and calculated, will be presented. In the theoretical calculation, Binary-Encounter-Bethe (BEB) model [18,19] is used, with its input quantities obtained from ab initio calculations. Fourier-transform mass spectrometry (FTMS) is used in experiments to measure the total and partial ionization cross sections of MCH. The kinetics of the reactions of MCH with selected hydrocarbon cations formed by electron ionization of MCH is studied using FTMS, and the reaction mechanisms will be discussed.

## 2. Experimental [20]

In the ionization cross-section measurements, $C_7H_{14}$ (99+%, Aldrich) was mixed with Ar (99.999%, Matheson) in a pressure ratio of about 1:1 to a total pressure of ~20 Torr (~3 kPa), as determined by capacitance manometry. The mixture was then admitted through a precision leak valve (Varian variable leak valve) into a modified Extrel FTMS system, with hardware and methods that have been described in detail elsewhere [21–25]. Ions were formed by electron impact in a cubic ion cyclotron resonance trap cell (5 cm on a side) at pressures in the $10^{-7}$ Torr ($10^{-5}$ Pa) range. An electron gun (Kimball Physics ELG2, Wilton, NH) irradiated the cell with a few hundred picocoulombs of electrons at a selected energy with

* Corresponding author.
*E-mail address:* steven.adams@wpafb.af.mil (S.F. Adams).

1387-3806/$ – see front matter © 2010 Published by Elsevier B.V.
doi:10.1016/j.ijms.2010.11.005

a spectral width of ±0.6 eV within the energy range of 10–200 eV. The motions of the product ions were constrained radially by the superconducting magnetic field (~2 Tesla) and axially by an electrostatic potential (trapping potential) applied to the trap faces that were perpendicular to the magnetic field. Ions of all mass-to-charge ratios, in a range of 10–500 amu (note: $H^+$ is therefore not detectable in our experiments), were simultaneously and coherently excited into cyclotron orbits using Stored Waveform Inverse Fourier Transform (SWIFT) [26–28] applied to two opposing trap faces which were parallel to the magnetic field. Following cyclotron excitation, the image currents induced on the two remaining faces of the trap were amplified, digitized and Fourier analyzed to yield a mass spectrum. In this study, the intensity ratios of the ions from $C_7H_{14}$ to $Ar^+$ gave cross sections relative to those for electron ionization of Ar [29], since the pressure ratio of $C_7H_{14}$ to Ar was known.

To study the subsequent reactions betweens ions and the parent molecule, a mixture of Ar and $C_7H_{14}$ or $C_7D_{14}$ (99 atom%, Aldrich, for the isotopic reaction study) with a pressure ratio of ~20:1 was used. The ion to be studied was selected by using SWIFT to eject other ions out of the trapping cell, followed by a cooling period in which the ion underwent multiple collisions with Ar at a total pressure of $\sim 1 \times 10^{-5}$ Torr (~1 mPa) for various times, typically 500 ms. SWIFT was used again to select the ion to be studied from others that were formed during the cooling period, followed by a programmed reaction time selectable typically from 0 to 4000 ms. The pressure of Ar and the length of the cooling period were adjusted so that at the end of the cooling period there were still sufficient reactant ions to study and their reaction showed a single exponential decay to the end of the reaction time at which only a few percent of the reactant ions were left over. With the high Ar partial pressure, $Ar^+$ was overpopulated during electron ionization, resulting in a significant space charge effect. To eliminate this effect, an rf waveform with the appropriate single-frequency for $Ar^+$ cyclotron resonance was applied during the electron beam event to continuously and selectively eject $Ar^+$ out of the trapping cell.

## 3. Computational details [20]

The Binary-Encounter-Bethe (BEB) model [18,19] has been shown to produce reliable total ionization cross-sections for a wide variety of molecules [30,31]. However, the model makes no predictions about ion fragmentation, that is, about partial cross-sections. An empirical study of ethylene suggests a correlation between orbital contributions and ion fragmentation [32], but this cannot yet be generalized or used predictively.

Input quantities for the BEB model (molecular orbital binding energies and kinetic energies) were obtained from ab initio calculations. Geometries were optimized using the hybrid B3LYP density functional [33,34], along with 6-31G(d) basis sets. All harmonic vibrational frequencies were real-valued. Orbital kinetic and binding energies were obtained from Hartree-Fock wavefunctions obtained with 6-311G(d,p) basis sets. Contingent upon pole strength (at least 0.8), valence orbital binding energies were refined using the outer-valence Green's function (OVGF) method [35,36] in conjunction with 6-311+G(d,p) basis sets. The binding energy for the highest occupied orbital, that is, the vertical ionization energy ($IE_v$) of the molecule, was obtained from frozen-core coupled-cluster computations [CCSD(T)] [37] with cc-pVTZ basis sets [38]. Several measurements of the adiabatic ionization energy have been reported (in eV): 9.85 ± 0.03 [39], 9.76 ± 0.03 [40], 9.69 ± 0.05 [41], 9.64 ± 0.05 [42], and 9.62 ± 0.05 [43]. For comparison with these experimental values, the present CCSD(T)/cc-pVTZ//B3LYP/6-31G(d) method yields an adiabatic value $IE_a$ = 9.65 eV (including vibrational zero-point energy scaled by 0.9757) [44]. However, no experimental value is available for $IE_v$, the necessary quantity in the BEB calculations.

**Table 1**
Orbital binding energies ($B$) and kinetic energies ($U$) for methylcyclohexane in its equatorial-chair conformation. All values in eV.

| Orbital | $B$ (eV) | $U$ (eV) |
|---|---|---|
| 1a′ | 305.35[a] | 436.06 |
| 2a′ | 305.19[a] | 435.90 |
| 1a″ | 305.18[a] | 436.00 |
| 3a′ | 305.16[a] | 436.15 |
| 2a″ | 305.14[a] | 436.08 |
| 4a′ | 305.14[a] | 436.12 |
| 5a′ | 305.03[a] | 436.03 |
| 6a′ | 30.34[a] | 33.67 |
| 7a′ | 23.73[b] | 35.62 |
| 3a″ | 23.06[b] | 36.22 |
| 8a′ | 21.83[c] | 36.05 |
| 4a″ | 19.87[c] | 35.16 |
| 9a′ | 19.22[c] | 35.43 |
| 10a′ | 18.23[c] | 28.68 |
| 11a′ | 15.77[c] | 24.67 |
| 12a′ | 15.02[c] | 25.50 |
| 13a′ | 14.78[c] | 28.10 |
| 5a″ | 14.79[c] | 25.68 |
| 6a″ | 14.00[c] | 27.79 |
| 14a′ | 13.24[c] | 28.11 |
| 7a″ | 12.86[c] | 30.51 |
| 15a′ | 12.55[c] | 32.13 |
| 8a″ | 12.01[c] | 34.05 |
| 9a″ | 11.85[c] | 30.59 |
| 16a′ | 11.59[c] | 30.62 |
| 17a′ | 11.09[c] | 29.18 |
| 18a′ | 10.45[c] | 37.51 |
| 10a″ | 10.51[d] | 35.94 |

[a] Koopmans.
[b] OVGF second-order pole.
[c] OVGF third-order pole.
[d] CCSD(T).

The threshold for double ionization ($IE_2$) was estimated by adding $IE_v$ of the neutral molecule to the energy for ionizing the resulting cation, still held at the geometry of the neutral precursor ($IE_{v2}$). The value of $IE_{v2}$ was obtained from OVGF/6-311+G(d,p) calculations, considering both singlet and triplet dications. Double ionization is presumed to occur whenever possible by a purely Auger mechanism, and the corresponding contribution to the cross-section is doubled because the dications are presumed to fragment into two singly-charged cations. Triple and higher ionizations are minor and are not considered. All computations were made using the Gaussian03 program [45].

The most stable conformation of methylcyclohexane is the chair (point group $C_s$) with the methyl group in an equatorial position. The axial-chair conformation has a Gibbs energy higher by only 7.5 kJ/mol at 298 K [46], [8.0 kJ/mol when computed using the composite G3(MP2) model [47]] so will make a small contribution (~5%) to the experimental measurement. However, our computed ionization cross-section is only about 1% larger for the axial conformer than for the equatorial, an insignificant difference. The equatorial-boat conformation lies at 24.6 kJ/mol [from G3(MP2) calculation] and is not significantly populated. Thus, we report molecular data (Table 1) only for the dominant, equatorial-chair conformation.

## 4. Results and discussion

### 4.1. Electron ionization

Table 2 lists the total cross section and partial cross sections for major channels of the dissociative ionization of MCH in an electron energy range of 10–200 eV. The major channels include the formation of cations of composition $C_2H_{3-5}$, $C_3H_{3,5,7}$, $C_4H_{5-9}$, $C_5H_{7-10}$, $C_6H_{10-12}$ and $C_7H_{13,14}$, which have cross sections greater than $10^{-17}$ cm$^2$ at 70 eV. Minor ions such as $CH_3^+$ are observed but

**Table 2**
Total and partial cross sections for major channels of electron ionization of MCH as functions of electron energy, in unit of $10^{-16}$ cm$^2$. Combined with the uncertainty in the reference cross-section of Ar for calibration, the estimated uncertainty is ±18%.

| Energy | $C_2H_3^+$ | $C_2H_4^{+\bullet}$ | $C_2H_5^+$ | $C_3H_3^+$ | $C_3H_5^+$ | $C_3H_6^{+\bullet}$ | $C_3H_7^+$ | $C_4H_5^+$ | $C_4H_6^{+\bullet}$ | $C_4H_7^+$ | $C_4H_8^{+\bullet}$ |
|---|---|---|---|---|---|---|---|---|---|---|---|
| 10 | | | | | | | | | | | |
| 11 | | | | | | | | | | <$10^{-3}$ | 0.001 |
| 12 | | | | | <$10^{-3}$ | 0.001 | | | <$10^{-3}$ | 0.002 | 0.004 |
| 13 | 0.001 | | <$10^{-3}$ | 0.001 | 0.003 | 0.002 | 0.001 | <$10^{-3}$ | 0.001 | 0.010 | 0.012 |
| 14 | 0.001 | 0.001 | 0.001 | 0.002 | 0.003 | 0.005 | 0.001 | 0.001 | 0.003 | 0.033 | 0.025 |
| 15 | 0.001 | 0.001 | 0.001 | 0.003 | 0.007 | 0.012 | 0.002 | 0.001 | 0.005 | 0.072 | 0.043 |
| 16 | 0.002 | 0.001 | 0.002 | 0.003 | 0.016 | 0.024 | 0.004 | 0.001 | 0.007 | 0.13 | 0.064 |
| 17 | 0.004 | 0.002 | 0.004 | 0.005 | 0.030 | 0.041 | 0.007 | 0.002 | 0.010 | 0.21 | 0.092 |
| 18 | 0.006 | 0.003 | 0.006 | 0.006 | 0.056 | 0.067 | 0.013 | 0.002 | 0.014 | 0.33 | 0.13 |
| 19 | 0.009 | 0.005 | 0.010 | 0.009 | 0.11 | 0.11 | 0.020 | 0.004 | 0.022 | 0.54 | 0.20 |
| 20 | 0.013 | 0.007 | 0.016 | 0.011 | 0.16 | 0.16 | 0.030 | 0.006 | 0.030 | 0.75 | 0.26 |
| 21 | 0.015 | 0.009 | 0.026 | 0.013 | 0.23 | 0.22 | 0.041 | 0.010 | 0.038 | 0.97 | 0.32 |
| 22 | 0.018 | 0.011 | 0.038 | 0.019 | 0.31 | 0.27 | 0.052 | 0.015 | 0.047 | 1.2 | 0.37 |
| 23 | 0.021 | 0.013 | 0.053 | 0.027 | 0.39 | 0.32 | 0.062 | 0.022 | 0.058 | 1.4 | 0.42 |
| 24 | 0.023 | 0.015 | 0.073 | 0.041 | 0.48 | 0.36 | 0.074 | 0.031 | 0.070 | 1.5 | 0.46 |
| 25 | 0.027 | 0.017 | 0.095 | 0.059 | 0.57 | 0.41 | 0.086 | 0.041 | 0.081 | 1.8 | 0.51 |
| 26 | 0.031 | 0.021 | 0.12 | 0.084 | 0.66 | 0.45 | 0.095 | 0.053 | 0.092 | 1.9 | 0.54 |
| 27 | 0.039 | 0.026 | 0.14 | 0.12 | 0.74 | 0.48 | 0.10 | 0.067 | 0.10 | 2.0 | 0.55 |
| 28 | 0.054 | 0.026 | 0.17 | 0.15 | 0.82 | 0.50 | 0.11 | 0.081 | 0.12 | 2.1 | 0.58 |
| 29 | 0.067 | 0.030 | 0.19 | 0.19 | 0.87 | 0.52 | 0.12 | 0.095 | 0.13 | 2.3 | 0.60 |
| 30 | 0.084 | 0.035 | 0.21 | 0.23 | 0.93 | 0.54 | 0.12 | 0.11 | 0.13 | 2.3 | 0.59 |
| 32 | 0.13 | 0.051 | 0.27 | 0.32 | 1.1 | 0.59 | 0.13 | 0.13 | 0.15 | 2.4 | 0.62 |
| 34 | 0.16 | 0.063 | 0.30 | 0.40 | 1.2 | 0.62 | 0.13 | 0.15 | 0.16 | 2.5 | 0.65 |
| 36 | 0.201 | 0.075 | 0.33 | 0.48 | 1.3 | 0.66 | 0.14 | 0.17 | 0.17 | 2.6 | 0.67 |
| 38 | 0.25 | 0.089 | 0.36 | 0.55 | 1.3 | 0.69 | 0.16 | 0.19 | 0.17 | 2.7 | 0.69 |
| 40 | 0.27 | 0.10 | 0.39 | 0.62 | 1.4 | 0.72 | 0.16 | 0.20 | 0.18 | 2.8 | 0.71 |
| 42 | 0.31 | 0.11 | 0.39 | 0.69 | 1.5 | 0.74 | 0.17 | 0.21 | 0.18 | 2.8 | 0.70 |
| 44 | 0.34 | 0.12 | 0.41 | 0.74 | 1.5 | 0.74 | 0.17 | 0.22 | 0.18 | 2.9 | 0.71 |
| 46 | 0.37 | 0.13 | 0.41 | 0.79 | 1.5 | 0.75 | 0.17 | 0.23 | 0.18 | 2.9 | 0.71 |
| 48 | 0.39 | 0.14 | 0.42 | 0.83 | 1.5 | 0.76 | 0.17 | 0.24 | 0.18 | 2.9 | 0.72 |
| 50 | 0.41 | 0.15 | 0.43 | 0.87 | 1.5 | 0.79 | 0.17 | 0.24 | 0.19 | 2.9 | 0.72 |
| 55 | 0.45 | 0.15 | 0.45 | 0.96 | 1.6 | 0.80 | 0.16 | 0.24 | 0.18 | 3.0 | 0.74 |
| 60 | 0.48 | 0.17 | 0.46 | 1.0 | 1.6 | 0.82 | 0.17 | 0.25 | 0.18 | 3.0 | 0.75 |
| 65 | 0.51 | 0.18 | 0.46 | 1.1 | 1.6 | 0.82 | 0.17 | 0.25 | 0.18 | 3.0 | 0.75 |
| 70 | 0.52 | 0.18 | 0.45 | 1.0 | 1.6 | 0.81 | 0.17 | 0.25 | 0.18 | 3.0 | 0.75 |
| 75 | 0.54 | 0.18 | 0.45 | 1.1 | 1.6 | 0.81 | 0.16 | 0.24 | 0.18 | 3.0 | 0.75 |
| 80 | 0.54 | 0.18 | 0.44 | 1.1 | 1.6 | 0.80 | 0.17 | 0.24 | 0.17 | 3.0 | 0.74 |
| 90 | 0.53 | 0.19 | 0.45 | 1.1 | 1.6 | 0.81 | 0.16 | 0.23 | 0.17 | 2.9 | 0.72 |
| 100 | 0.53 | 0.18 | 0.44 | 1.0 | 1.6 | 0.79 | 0.16 | 0.23 | 0.17 | 2.8 | 0.71 |
| 110 | 0.52 | 0.18 | 0.43 | 1.0 | 1.6 | 0.78 | 0.16 | 0.22 | 0.16 | 2.8 | 0.70 |
| 120 | 0.50 | 0.18 | 0.42 | 1.0 | 1.5 | 0.76 | 0.15 | 0.22 | 0.16 | 2.8 | 0.69 |
| 130 | 0.48 | 0.16 | 0.40 | 0.97 | 1.5 | 0.75 | 0.17 | 0.20 | 0.15 | 2.7 | 0.68 |
| 140 | 0.49 | 0.16 | 0.40 | 0.95 | 1.4 | 0.75 | 0.17 | 0.20 | 0.15 | 2.7 | 0.67 |
| 150 | 0.48 | 0.15 | 0.40 | 0.92 | 1.4 | 0.74 | 0.16 | 0.20 | 0.15 | 2.7 | 0.67 |
| 160 | 0.46 | 0.15 | 0.39 | 0.89 | 1.4 | 0.73 | 0.14 | 0.19 | 0.15 | 2.6 | 0.66 |
| 170 | 0.43 | 0.13 | 0.35 | 0.86 | 1.3 | 0.68 | 0.12 | 0.20 | 0.15 | 2.6 | 0.63 |
| 180 | 0.42 | 0.13 | 0.35 | 0.86 | 1.3 | 0.68 | 0.12 | 0.19 | 0.15 | 2.5 | 0.63 |
| 190 | 0.41 | 0.13 | 0.34 | 0.83 | 1.3 | 0.66 | 0.12 | 0.19 | 0.14 | 2.5 | 0.62 |
| 200 | 0.40 | 0.12 | 0.33 | 0.82 | 1.3 | 0.65 | 0.12 | 0.18 | 0.14 | 2.4 | 0.61 |

| Energy | $C_4H_9^+$ | $C_5H_7^+$ | $C_5H_8^{+\bullet}$ | $C_5H_9^+$ | $C_5H_{10}^{+\bullet}$ | $C_6H_{10}^{+\bullet}$ | $C_6H_{11}^+$ | $C_6H_{12}^{+\bullet}$ | $C_7H_{13}^+$ | $C_7H_{14}^{+\bullet}$ | Total |
|---|---|---|---|---|---|---|---|---|---|---|---|
| 10 | | | | | | <$10^{-3}$ | <$10^{-3}$ | | | 0.006 | 0.007 |
| 11 | | | 0.001 | | 0.003 | 0.005 | 0.008 | 0.001 | | 0.037 | 0.055 |
| 12 | 0.001 | 0.001 | 0.003 | 0.002 | 0.010 | 0.018 | 0.044 | 0.003 | 0.001 | 0.084 | 0.18 |
| 13 | 0.003 | 0.002 | 0.008 | 0.009 | 0.025 | 0.038 | 0.11 | 0.007 | 0.003 | 0.14 | 0.39 |
| 14 | 0.006 | 0.006 | 0.015 | 0.020 | 0.043 | 0.059 | 0.19 | 0.012 | 0.006 | 0.21 | 0.65 |
| 15 | 0.009 | 0.010 | 0.023 | 0.035 | 0.065 | 0.084 | 0.29 | 0.017 | 0.011 | 0.28 | 0.98 |
| 16 | 0.013 | 0.015 | 0.032 | 0.052 | 0.088 | 0.10 | 0.39 | 0.023 | 0.016 | 0.35 | 1.3 |
| 17 | 0.018 | 0.023 | 0.043 | 0.075 | 0.12 | 0.13 | 0.52 | 0.031 | 0.023 | 0.45 | 1.9 |
| 18 | 0.025 | 0.034 | 0.058 | 0.11 | 0.16 | 0.17 | 0.68 | 0.042 | 0.033 | 0.59 | 2.6 |
| 19 | 0.036 | 0.053 | 0.083 | 0.16 | 0.22 | 0.25 | 0.97 | 0.063 | 0.050 | 0.81 | 3.8 |
| 20 | 0.047 | 0.072 | 0.11 | 0.21 | 0.29 | 0.31 | 1.2 | 0.080 | 0.066 | 1.0 | 4.9 |
| 21 | 0.055 | 0.091 | 0.13 | 0.25 | 0.34 | 0.36 | 1.4 | 0.093 | 0.081 | 1.2 | 5.9 |
| 22 | 0.064 | 0.11 | 0.14 | 0.29 | 0.38 | 0.40 | 1.6 | 0.11 | 0.098 | 1.3 | 6.9 |
| 23 | 0.071 | 0.13 | 0.16 | 0.32 | 0.42 | 0.45 | 1.8 | 0.12 | 0.11 | 1.4 | 7.9 |
| 24 | 0.077 | 0.15 | 0.17 | 0.35 | 0.45 | 0.48 | 1.9 | 0.13 | 0.13 | 1.5 | 8.7 |
| 25 | 0.084 | 0.17 | 0.19 | 0.39 | 0.49 | 0.51 | 2.0 | 0.13 | 0.14 | 1.6 | 9.5 |
| 26 | 0.090 | 0.18 | 0.20 | 0.41 | 0.51 | 0.53 | 2.1 | 0.14 | 0.16 | 1.7 | 10.3 |
| 27 | 0.092 | 0.20 | 0.21 | 0.42 | 0.52 | 0.53 | 2.2 | 0.14 | 0.16 | 1.7 | 10.8 |
| 28 | 0.094 | 0.21 | 0.21 | 0.43 | 0.53 | 0.55 | 2.3 | 0.14 | 0.17 | 1.8 | 11.3 |
| 29 | 0.10 | 0.22 | 0.22 | 0.45 | 0.55 | 0.55 | 2.3 | 0.14 | 0.19 | 1.9 | 11.9 |
| 30 | 0.10 | 0.23 | 0.22 | 0.45 | 0.55 | 0.56 | 2.3 | 0.15 | 0.19 | 1.9 | 12.1 |

**Table 2**
(*Continued*)

| Energy | $C_4H_9^+$ | $C_5H_7^+$ | $C_5H_8^{+\bullet}$ | $C_5H_9^+$ | $C_5H_{10}^{+\bullet}$ | $C_6H_{10}^{+\bullet}$ | $C_6H_{11}^+$ | $C_6H_{12}^{+\bullet}$ | $C_7H_{13}^+$ | $C_7H_{14}^{+\bullet}$ | Total |
|---|---|---|---|---|---|---|---|---|---|---|---|
| 32 | 0.11 | 0.25 | 0.23 | 0.46 | 0.56 | 0.57 | 2.4 | 0.16 | 0.22 | 1.9 | 13.1 |
| 34 | 0.11 | 0.27 | 0.24 | 0.49 | 0.59 | 0.58 | 2.5 | 0.16 | 0.24 | 2.0 | 13.7 |
| 36 | 0.11 | 0.28 | 0.24 | 0.50 | 0.60 | 0.59 | 2.5 | 0.17 | 0.25 | 2.0 | 14.4 |
| 38 | 0.11 | 0.29 | 0.25 | 0.51 | 0.61 | 0.60 | 2.6 | 0.17 | 0.27 | 2.0 | 15.0 |
| 40 | 0.12 | 0.30 | 0.25 | 0.52 | 0.62 | 0.62 | 2.6 | 0.17 | 0.29 | 2.1 | 15.5 |
| 42 | 0.12 | 0.30 | 0.26 | 0.53 | 0.63 | 0.61 | 2.6 | 0.17 | 0.30 | 2.1 | 15.9 |
| 44 | 0.12 | 0.31 | 0.26 | 0.53 | 0.63 | 0.62 | 2.7 | 0.18 | 0.30 | 2.1 | 16.2 |
| 46 | 0.12 | 0.31 | 0.26 | 0.54 | 0.63 | 0.62 | 2.7 | 0.17 | 0.31 | 2.1 | 16.4 |
| 48 | 0.12 | 0.31 | 0.26 | 0.54 | 0.64 | 0.61 | 2.7 | 0.18 | 0.32 | 2.1 | 16.6 |
| 50 | 0.12 | 0.31 | 0.26 | 0.56 | 0.65 | 0.63 | 2.7 | 0.18 | 0.33 | 2.2 | 16.9 |
| 55 | 0.12 | 0.31 | 0.26 | 0.55 | 0.65 | 0.63 | 2.7 | 0.18 | 0.33 | 2.2 | 17.2 |
| 60 | 0.12 | 0.33 | 0.27 | 0.56 | 0.66 | 0.63 | 2.7 | 0.17 | 0.34 | 2.2 | 17.5 |
| 65 | 0.13 | 0.33 | 0.27 | 0.55 | 0.64 | 0.63 | 2.7 | 0.18 | 0.36 | 2.2 | 17.7 |
| 70 | 0.13 | 0.32 | 0.27 | 0.54 | 0.64 | 0.62 | 2.7 | 0.16 | 0.36 | 2.1 | 17.5 |
| 75 | 0.12 | 0.30 | 0.25 | 0.55 | 0.63 | 0.62 | 2.6 | 0.16 | 0.34 | 2.1 | 17.5 |
| 80 | 0.12 | 0.30 | 0.25 | 0.54 | 0.63 | 0.61 | 2.6 | 0.18 | 0.34 | 2.1 | 17.4 |
| 90 | 0.12 | 0.30 | 0.25 | 0.55 | 0.64 | 0.62 | 2.6 | 0.18 | 0.35 | 2.1 | 17.4 |
| 100 | 0.12 | 0.29 | 0.24 | 0.53 | 0.61 | 0.61 | 2.6 | 0.17 | 0.35 | 2.1 | 17.0 |
| 110 | 0.12 | 0.30 | 0.25 | 0.52 | 0.61 | 0.60 | 2.5 | 0.17 | 0.35 | 2.0 | 16.9 |
| 120 | 0.12 | 0.29 | 0.24 | 0.51 | 0.59 | 0.57 | 2.4 | 0.16 | 0.33 | 2.0 | 16.4 |
| 130 | 0.11 | 0.28 | 0.23 | 0.50 | 0.57 | 0.56 | 2.4 | 0.16 | 0.32 | 2.0 | 16.1 |
| 140 | 0.11 | 0.27 | 0.23 | 0.49 | 0.57 | 0.56 | 2.4 | 0.16 | 0.32 | 1.9 | 15.9 |
| 150 | 0.11 | 0.27 | 0.23 | 0.49 | 0.57 | 0.55 | 2.4 | 0.17 | 0.31 | 1.9 | 15.7 |
| 160 | 0.11 | 0.26 | 0.22 | 0.49 | 0.57 | 0.54 | 2.3 | 0.16 | 0.30 | 1.9 | 15.4 |
| 170 | 0.11 | 0.27 | 0.23 | 0.48 | 0.55 | 0.53 | 2.3 | 0.14 | 0.29 | 1.8 | 14.9 |
| 180 | 0.11 | 0.26 | 0.22 | 0.47 | 0.54 | 0.52 | 2.3 | 0.14 | 0.29 | 1.8 | 14.7 |
| 190 | 0.11 | 0.26 | 0.22 | 0.46 | 0.54 | 0.52 | 2.2 | 0.14 | 0.29 | 1.8 | 14.4 |
| 200 | 0.11 | 0.26 | 0.22 | 0.46 | 0.53 | 0.51 | 2.2 | 0.14 | 0.28 | 1.8 | 14.3 |

are not shown in the table because of their very insignificant values. The total ionization cross section reaches a broad maximum of $17.7 \times 10^{-16}$ cm$^2$ at ~65 eV. Branching ratios of some major ionization products, derived from their cross section data, are shown in Fig. 1, for the purpose of demonstrating the composition changes in the ion population. The parent ion $C_7H_{14}^{+\bullet}$ is significantly present throughout the energy range studied. Its branching ratio, however, drops dramatically from 10 to 30 eV, yielding dominance to the fragment ion $C_6H_{11}^+$ and then to $C_4H_7^+$ at elevated energies. The most abundant ions at energies below 20 eV are basically the parent ions and $C_6H_{11}^+$. At higher energies $C_4H_7^+$ becomes more important and is the most abundant ion above 30 eV. An examination of the data of $C_6H_{10}^{+\bullet}$ and $C_6H_{11}^+$ shows that at 10 eV the branching ratio of $C_6H_{10}^{+\bullet}$ is greater than $C_6H_{11}^+$, but at higher energies the order reverses. The crossing in the branching ratio curves of these two ions indicates that the reactions forming these two ions are parallel and competing with each other. While $C_6H_{11}^+$ results from a simple single-bond cleavage eliminating the methyl from $C_7H_{14}^{+\bullet}$, which has a characteristic cross section with a higher onset energy but a faster rise, $C_6H_{10}^{+\bullet}$ results from bond cleavages with rearrangement eliminating a methane molecule from the parent ion, which has a cross section with a lower onset energy but rises slower. These are common characteristics for competing simple cleavage vs. rearrangement reactions [48].

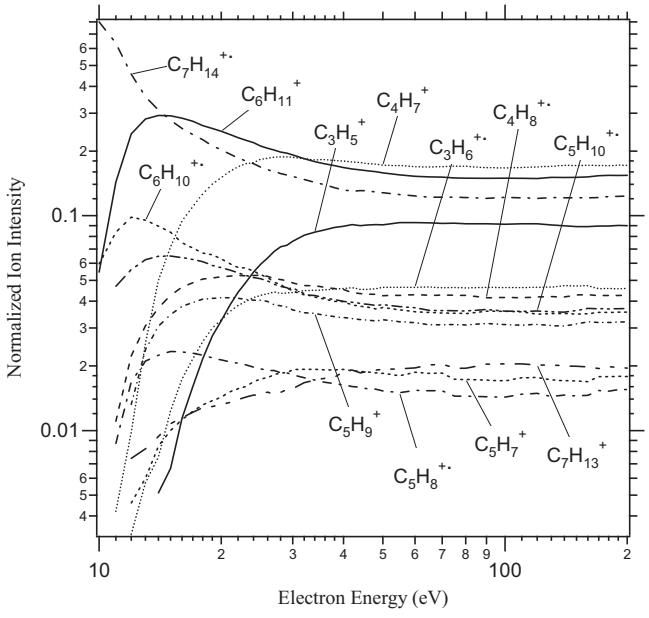


**Fig. 1.** Log–log plot of branching ratios of major product ions from electron ionization of methylcyclohexane, the normalized partial cross sections of these ions over the total ionization cross section.

The computed total ionization cross-sections are summarized in Table 3 and are compared with the experimental data in Fig. 2. The maximum value is $21.0 \times 10^{-16}$ cm$^2$, at an incident electron energy of 70 eV. This exceeds our measured value by $3 \times 10^{-16}$ cm$^2$, or ~20%. The BEB cross-section is sensitive to the value of the ionization threshold, but no reasonable choices can decrease the peak cross-section so much. For example, using binding energies of 11.5 eV for the three highest orbitals (17a′, 18a′, and 10a″) lowers the peak cross-section only to $20.5 \times 10^{-16}$ cm$^2$ (at 75 eV).

To test the computational procedure on a related molecule, we performed analogous calculations on propane ($C_3H_8$). We obtain a peak BEB cross-section of $9.6 \times 10^{-16}$ cm$^2$ (at 70 eV). This agrees well (discrepancies of +10% and −6%, respectively) with the available experimental values of $8.75 \times 10^{-16}$ cm$^2$ (90 eV)[49] and $10.24 \times 10^{-16}$ cm$^2$ (90 eV) [50]. Schram et al. measured cross-sections for several hydrocarbons at high energies (0.6–12 keV) [51]. At 600 eV, our computed cross-section for propane, $3.68 \times 10^{-16}$ cm$^2$, is 11% lower than their measured value, $4.13 \times 10^{-16}$ cm$^2$. Thus, our computation for propane appears to be reliable.

The uncertainty in the FTMS measurements is estimated to be ±14%. Combined with the uncertainty of ±3.5% in the Ar cross section used for calibration [29], the overall uncertainty in the measured cross sections reported in this paper is ±18%. The slightly lower values of the experimental data compared to the theoretical

**Table 3**
Total ionization cross-section for methylcyclohexane, from BEB calculations. Units are eV for incident electron energy ($T$) and $10^{-16}$ cm$^2$ for cross-section ($\sigma$).

| $T$/(eV) | $\sigma$/($10^{-16}$ cm$^2$) |
|---|---|
| 10.45 | 0 |
| 11 | 0.11 |
| 12 | 0.48 |
| 13 | 1.1 |
| 14 | 1.9 |
| 15 | 2.8 |
| 16 | 3.8 |
| 17 | 4.9 |
| 18 | 5.8 |
| 19 | 6.8 |
| 20 | 7.7 |
| 22 | 9.4 |
| 24 | 10.9 |
| 26 | 12.3 |
| 28 | 13.5 |
| 30 | 14.6 |
| 35 | 16.7 |
| 40 | 18.2 |
| 45 | 19.3 |
| 50 | 20.0 |
| 60 | 20.8 |
| 70 | 21.0 |
| 80 | 21.0 |
| 90 | 20.7 |
| 100 | 20.3 |
| 125 | 19.2 |
| 150 | 18.0 |
| 200 | 15.9 |
| 600 | 8.1 |

data is most likely due to the missing partial cross section for proton formation. If we compare with the relative intensities measured by Wang and Vidal [52] for propane at 200 eV, this feature could add at least 6% to the total cross sections.

The formation of certain doubly-charged cations, such as $C_4H_7^{2+}$ and $C_6H_{11}^{2+}$ at $m/z$ 27.5 and 41.5, respectively, has been observed. Their branching ratios, based on the number of charges, have an upper limit of only 0.25%, however. Other possible doubly-charged ions are superimposed in mass spectra with their isobar ions that

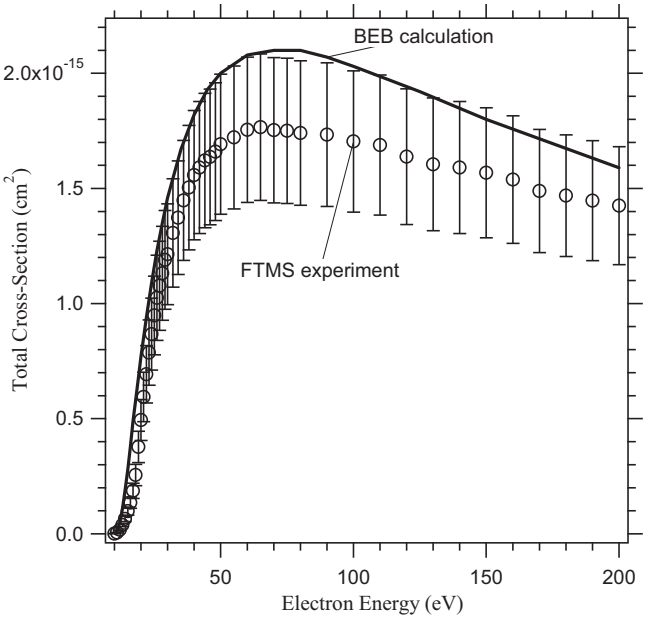


**Fig. 2.** Comparison of the total ionization cross sections measured by FTMS experiment (symbols with error bars) and calculated using BEB model (solid line). Error bars indicate ±18% uncertainty in FTMS measurements.

are singly-charged and have half of the mass, and therefore cannot be determined. Investigation of a possible method to distinguish the contributions of the singly- and doubly-charged ions, by using ion-neutral reactions to "titrate" the doubly-charged ions, is underway.

### 4.2. Ion-molecule reactions

Previous studies on ion molecule reactions of MCH with inorganic ions, including $O_2^{+\bullet}$, $NO^+$, $H_3O^+$, $H_3^+$ and $N_2H^+$, show three types of reactions: charge transfer, hydride ($H^-$) transfer and proton ($H^+$) transfer [13,15,16]. In our study, we investigated the reactions between MCH and selected hydrocarbon ions that are major products from the electron ionization of MCH, with the results shown in Table 4. As is discussed in detail later, the major reactions observed include charge transfer forming $C_7H_{14}^{+\bullet}$ and hydride transfer forming $C_7H_{13}^+$, but no proton transfer. In addition, some odd-electron reactant ions ($C_xH_{2y}^{+\bullet}$) are found to undergo $H_2^{-\bullet}$ transfer forming $C_7H_{12}^{+\bullet}$. Table 4 lists the reactant ions, in the order of the increasing ion masses, their possible structural isomers, product ions and their branching ratios, the enthalpies of reaction, and the rate constants. The enthalpies of reaction are provided for all ions' charge transfer and hydride transfer reactions, regardless whether the reaction is actually observed, for the purpose of discussing their reactivity in relation to their enthalpies of reaction. In addition, for all odd-electron ions, data for the $H_2^{-\bullet}$ transfer reactions are provided as well. The enthalpies of reaction are calculated using literature thermochemical data or theoretically computed using G3(MP2) [47] calculations when literature data are not available. The listed isomers may not be exhaustive, but they represent most of the reasonable structures of the reactant ions. In calculating the enthalpies of reaction, the structures of the ionic and neutral products are assumed to be as derived from the reactant structures, with minimum atom rearrangements if any. The relative rate constants for most ion reactions are obtained by fitting the time-dependent ion intensities using the reaction model of a single isomer reactant ion forming product ions in a parallel manner. This single isomer fitting technique is found to work well for most ions, except for reactions involving $C_3H_6^{+\bullet}$ and $C_4H_8^{+\bullet}$. A typical set of data for a single isomer reaction is shown in Fig. 3a, from which it can be seen that the decay of the reactant ion is single-exponential, and the ratio of product ion intensities remains constant throughout most of the reaction time. This type of reaction kinetics usually indicates that there is only one isomer in the reactant ion population or, if there are more isomers, their reactivities are similar. The reactions of $C_3H_6^{+\bullet}$ and $C_4H_8^{+\bullet}$ are the exception, as is shown in Fig. 3b for the data of $C_4H_8^{+\bullet}$ as an example. The decay of the $C_4H_8^{+\bullet}$ reactant ion is not single-exponential and, more obviously, the ratio of the product ion intensities is not constant over the reaction time. We explain this type of reaction kinetics as due to two or more isomers in the reactant ion population that have different reactivities, as is discussed in more detail below. The absolute rate constants, listed in Table 4 as $k_{exp.}$, are the results of the data fitting, calibrated against the decay rate of $O_2^{+\bullet}$ in its reaction with MCH under the same gas pressure, which has a known reaction rate constant reported by Midey et al. [13] The collision rate constants, $k_{coll.}$, are calculated using Langevin theory with the polarizability of MCH as $13.1 \times 10^{-24}$ cm$^3$ [53].

### 4.3. Reactions of even-electron ions

Even-electron ions ($C_xH_{2y+1}^+$), expected to have closed-shell electronic structures, tend to be more stable than the odd-electron radical cations ($C_xH_{2y}^{+\bullet}$). As seen in Table 4, all even-electron ions, except $C_3H_3^+$, $C_4H_5^+$ and $C_5H_7^+$ which are totally unreactive, react

**Table 4**
Ion-molecule reactions of MCH with selected hydrocarbon ions formed in electron ionization of MCH. Product ions and their branching ratios (%) are listed. Measured reaction rate constants, $k_{exp.}$, and calculated collision rate constants, $k_{coll.}$, are given in the unit of $10^{-10}$ $cm^3/s$. Enthalpies of reaction ($\Delta H_{rxn}$, in kJ/mol) for the given possible structures of the reactant ions are provided.

| Reactant ion | Possible structure | Product ion branching ratio (%) $\Delta H_{rxn}$[a] | | | | $k_{exp.}$ | $k_{coll.}$ |
|---|---|---|---|---|---|---|---|
| | | $C_7H_{14}^{+\bullet}$ | $C_7H_{13}^{+}$ [b] | $C_7H_{12}^{+\bullet}$ [c] | $C_6H_x^{+}$ [d] | | |
| $C_2H_3^+$ | | 0% | 100% | | | 12 | 18 |
| | $CH_2$=CH | 83 | −250.1 | | | | |
| $C_2H_4^{+\bullet}$ | | 50% | 45% | 0% | 5% | 16 | 18 |
| | $CH_2$=$CH_2$ | −84.1 | −138.3 | −202 | −77.8[e] | | |
| $C_2H_5^+$ | | 0% | 100% | | | 10 | 18 |
| | $CH_3CH_2$ | 145.7 | −176.3 | | | | |
| $C_3H_3^+$ | | 0% | 0% | | | 0 | 16 |
| | $CH_2C$≡CH | 93.7 | −182.7 | | | | |
| | Cyclopropenyl | 294.7 | 11.7 | | | | |
| $C_3H_5^+$ | | 0% | 100% | | | 4.7 | 16 |
| | $CH_2CH$=$CH_2$ | 145.1 | −115.7 | | | | |
| | $CH_3C$=$CH_2$ | 225.0[f] | −139.1 | | | | |
| | Cyclopropyl | 140.6 | −206 | | | | |
| $C_3H_6^{+\bullet}$ (i) | | 0% | 69% | 31% | 0% | 9.1 | 16 |
| | $CH_3CH$=$CH_2$ | −9.1 | −56 | −115.5 | 14.5[g] | | |
| $C_3H_6^{+\bullet}$ (ii) | | 46% | 38% | 0% | 16% | 15 | 16 |
| | Cyclopropane | −21 | −93.8 | −160.5 | −23.3[g] | | |
| $C_4H_5^+$ | | 0% | 0% | | | 0 | 14 |
| | $CH_3C$≡$CCH_2$ | 162.7 | −100.9 | | | | |
| | HC≡$CCHCH_3$ | 160.7 | −99.1 | | | | |
| | $CH_2$=CCH=$CH_2$ | 226.6[f] | −109.3 | | | | |
| | Cyclobutenyl | 255.5[f] | −43.9[f] | | | | |
| | Methylcyclopropenyl | 410.9[f] | 88.1[f] | | | | |
| $C_4H_6^{+\bullet}$ | | 0% | 74% | 26% | | 4.0 | 14 |
| | $CH_2$=C=$CHCH_3$ | 59 | −90.7[h1] | −97.2[h2] | | | |
| | (E)-$CH_2$=CHCH=$CH_2$ | 54.7 | −42.7[h1] | −37.4 | | | |
| | CH≡$CCH_2CH_3$ | −52.1 | −97.8[f] | −199.4 | | | |
| | $CH_3C$≡$CCH_3$ | 7.1 | −23.9[f] | −132.2[h2] | | | |
| | cyclobutene | 19.4 | −43.1 | −90.6 | | | |
| | 1-methylcyclopropene | 75.6[f] | −48.3[f] | −151.6[f] | | | |
| | 3-methylcyclopropene | 41.3[f] | −83.7[f] | −199.2[f] | | | |
| | methylenecyclopropane | 36.6[f] | −73.8[f] | −153 | | | |
| $C_4H_7^+$ | | 0% | 100% | | | 3.5 | 14 |
| | $CH_3CHCH$=$CH_2$ | 217.3 | −35.7 | | | | |
| | $CH_2C(CH_3)$=$CH_2$ | 167.7 | −90.2 | | | | |
| | $CH_3C$=$CHCH_3$ | 254.5[f] | −95.5[h2] | | | | |
| | $CH_2$=$CHCH_2CH_2$ | 152.7 | −158.7 | | | | |
| | vinyl bridging ethylene | 280.9[f] | −49.5[f] | | | | |
| | cyclobutyl | 202.9 | −102.9 | | | | |
| $C_4H_8^{+\bullet}$ (i) | | 0% | 100% | 0% | | 0.83 | 14 |
| | $CH_3CH_2CH$=$CH_2$ | 5.3 | −43.3[h3] | −102.5 | | | |
| | $(CH_3)_2C$=$CH_2$ | 38.8 | −18.1[h4] | −60.5 | | | |
| $C_4H_8^{+\bullet}$ (ii) | | 0% | 0% | 100% | | 2.9 | 14 |
| | (Z)-$CH_3CH$=$CHCH_3$ | 50.9 | 9.7 | −49.5 | | | |
| | (E)-$CH_3CH$=$CHCH_3$ | 51.5 | 14.7 | −44.5 | | | |
| $C_4H_8^{+\bullet}$ (iii) | | | | | | | |
| | Cyclobutane | −26.9 | −101.3 | −163.5 | | | |
| $C_5H_7^+$ | | 0% | 0% | | | 0 | 13 |
| | $CH_2$=$CHCHCH$=$CH_2$ | 229.7 | −6.6 | | | | |
| | $CH_2$=$C(CH_2)CH$=$CH_2$ | 200.6[f] | −108.7[f] | | | | |
| | HC≡$CC(CH_3)_2$ | 211.7 | −35.3 | | | | |
| | CH≡$CCHCH_2CH_3$ | 204.5[f] | −86.6[f] | | | | |
| | $CH_3C$≡$CCHCH_3$ | 250.3[f] | −39.5[f] | | | | |
| | $CH_2C$≡$CCH_2CH_3$ | 203.5[f] | −95.5[f] | | | | |
| | Cyclopentenyl | 255.7 | 12.7 | | | | |
| $C_5H_8^{+\bullet}$ | | 0% | 0% | 100% | | 0.39 | 13 |
| | $CH_2$=C=$CHCH_2CH_3$ | 40.4 | −114.3[h5] | −108.5[h6] | | | |
| | (Z)-$CH_2$=CHCH=$CHCH_3$ | 96.8 | 1.7[h5] | 7.5[h6] | | | |
| | (E)-$CH_2$=CHCH=$CHCH_3$ | 101 | 10.7[h5] | 11.5[h7] | | | |
| | $CH_2$=$CHCH_2CH$=$CH_2$ | 1.4 | −34.3[f] | −103.4[h7] | | | |
| | $CH_3CH$=C=$CHCH_3$ | 90.8 | −70.3[h8] | −50.5[h6] | | | |
| | $CH_2$=$C(CH_3)CH$=$CH_2$ | 76.8 | −37.2[h9] | −7.3[h10] | | | |
| | $C_3H_7C$≡CH | −40.3 | −81.8[f] | −187.4 | | | |
| | $C_2H_5C$≡$CCH_3$ | 18.7 | −229.3[h11] | −122.5[h7] | | | |
| | $(CH_3)_2CHC$≡CH | −32.3 | −288.3[h12] | −177.4[h10] | | | |
| | $CH_2$=C=$C(CH_3)_2$ | 101.3[f] | −61.3[f] | −80.6[f] | | | |
| | Cyclopentene | 60.7 | 6.7[h13] | −35.4[h14] | | | |
| | 1-Methylcyclobutene | 92.7[f] | 24.8[f] | −45.9[f] | | | |
| | 3-Methylcyclobutene | 51.3[f] | −19.1[f] | −99.6[f] | | | |
| | Methylenecyclobutane | 45.7 | 1.1[f] | −63[h15] | | | |
| | Vinylcyclopropane | 90.7 | 45.0[f] | −45[h16] | | | |
| | Spiropentane | 36.8 | −47.0[f] | −138[h17] | | | |

**Table 4**
(*Continued*)

| Reactant ion | Possible structure | Product ion branching ratio (%) $\Delta H_{rxn}$[a] | | | | $k_{exp.}$ | $k_{coll.}$ |
|---|---|---|---|---|---|---|---|
| | | $C_7H_{14}^{+\bullet}$ | $C_7H_{13}^{+}$ [b] | $C_7H_{12}^{+\bullet}$ [c] | $C_6H_x^{+}$ [d] | | |
| $C_5H_9^+$ | | 0% | 100% | | | 0.26 | 13 |
| | $CH_2$=$CHCHCH_2CH_3$ | 225.7 | −21.7 | | | | |
| | (E)-$CH_3CHCH$=$CHCH_3$ | 258.7 | 15.2[h7] | | | | |
| | $CH_3CH$=$CC_2H_5$ | 264.9[f] | −59.8[h7] | | | | |
| | $(CH_3)_2CCH$=$CH_2$ | 243.7 | 15.3 | | | | |
| | $(CH_3)_2CHC$=$CH_2$ | 258.1[f] | −55.7 | | | | |
| | $CH_3CH$=$C(CH_3)CH_2$ | 255.1[f] | −29.4 | | | | |
| | $CH_2$=$C(CH_2)C_2H_5$ | 204.3[f] | −88.3[f] | | | | |
| | Cyclopentyl | 230.9 | −69.5 | | | | |
| | 1-Methylcyclobutyl | 320.4[f] | −10.9[f] | | | | |
| $C_5H_{10}^{+\bullet}$ | | 0% | 0% | 100% | | 0.086 | 13 |
| | $CH_2$=$CHCH_2CH_2CH_3$ | 11.3 | −37.3[h18] | −95.5 | | | |
| | (Z)-$CH_3CH_2CH$=$CHCH_3$ | 57.9 | 14.4[h18] | −43.8 | | | |
| | (E)-$CH_3CH_2CH$=$CHCH_3$ | 57.9 | 19.4[h18] | −38.8 | | | |
| | $(CH_3)_2CHCH$=$CH_2$ | 11.3 | −33.2[f] | ≤−96.8 | | | |
| | $C_2H_5C(CH_3)$=$CH_2$ | 49.1 | −8.3[h19] | ≤−50.8 | | | |
| | $(CH_3)_2C$=$CHCH_3$ | 92.6 | 41.7[h19] | ≤−0.8 | | | |
| | Cyclopentane | −84.7 | −70.3[h20] | −134.5[h21] | | | |
| | Methylcyclobutane | 3.7 | −50.8[f] | −122.9[f] | | | |
| $C_6H_{10}^{+\bullet}$ | | 0% | 0% | 100% | | 0.083 | 13 |
| | Cyclohexene | 66.7 | 28.3 | −33.7 | | | |
| $C_6H_{11}^+$ | | 0% | 100% | | | 1.4 | 13 |
| | Cyclohexyl | 273.7 | −46.6 | | | | |

[a] Enthalpies of reaction are calculated using thermochemical data from Ref. [55]. For the reactions of $C_4H_5^+$ and $C_4H_6^{+\bullet}$, additional thermochemical data are taken from Ref. [53] and [57].
[b] The product ion $C_7H_{13}^+$ is assumed to be 1-methyl-cyclohexylium.
[c] The product ion $C_7H_{12}^{+\bullet}$ is assumed to be 1-methyl-cyclohexene radical cation.
[d] $x$ = 11 or 9 for the reaction of $C_2H_4^{+\bullet}$ or $C_3H_6^{+\bullet}$, respectively.
[e] The products are assumed to be c-$C_6H_{11}^+$ and n-$C_3H_7$.
[f] Theoretical value from G3(MP2) calculations, for $T$ = 0 K.
[g] The product ion is assumed to be cyclohexenylium, formed by dissociative $H^{-\bullet}$ transfer; if it is formed by dissociative $H_2^{-\bullet}$ transfer, the $\Delta H_{rxn}$ values will be more endothermic (or less exothermic) by 22.5 kJ/mol for (i) and 15.3 kJ/mol for (ii) (see the text).
[h] The neutral product is assumed to be: (1) $CH_2$=$CHCHCH_3^{\bullet}$; (2) 2-(E)-$C_4H_8$; (3) $CH_3CHCH_2CH_3^{\bullet}$; (4) $^{\bullet}C(CH_3)_3$; (5) $CH_2$=$CHCHCH_2CH_3^{\bullet}$; (6) 2-(Z)-$C_5H_{10}$; (7) 2-(E)-$C_5H_{10}$; (8) (E)-$CH_3CHCH$=$CHCH_3^{\bullet}$; (9) $(CH_3)_2CCH$=$CH_2^{\bullet}$; (10) $(CH_3)_2CHCH$=$CH_2$; (11) $CH_3CH$=$CC_2H_5^{\bullet}$; (12) $(CH_3)_2CHC$=$CH_2^{\bullet}$; (13) cyclopentyl radical; (14) c-$C_5H_{10}$; (15) methylcyclobutane; (16) ethylcyclopropane; (17) 1,1-dimethylcyclopropane; (18) $CH_3CH_2CH_2CHCH_3^{\bullet}$; (19) $(CH_3)_2CCH_2CH_3^{\bullet}$; (20) 1-$C_5H_{11}^{\bullet}$; (21) n-$C_5H_{12}$.

with MCH only by hydride transfer forming $C_7H_{13}^+$:

$$A^+ + C_7H_{14} \rightarrow C_7H_{13}^+ + AH, (A^+: \text{even-electron ions}) \quad (1)$$

When isotope reagents are used, the isotope distribution of the product ion is exclusively determined by the isotope content of MCH, as shown below for the reaction of $C_2D_3^+$ as an example:

$$C_2D_3^+ + C_7H_{14} \rightarrow C_7H_{13}^+ + C_2D_3H. \quad (2)$$

No product ion containing a D atom is observed. This isotope distribution suggests that reaction (1) is not likely to occur through the dissociative proton transfer mechanism, which would give some retention of the incoming D atom in the product ions [54].

No charge transfer reaction forming $C_7H_{14}^{+\bullet}$ is observed for the even-electron ions, which is likely to be due to the fact that all such reactions are endothermic, as shown by the enthalpies of reaction listed in Table 4. The endothermicity of the charge transfer also rules out the possibility of reaction (1) as through a dissociative charge transfer mechanism.

The enthalpy of reaction calculations for all channels forming $C_7H_{13}^+$ listed in Table 4 are based on the assumption of the hydride transfer mechanism (1). It can be seen that all of the observed hydride transfer reactions of $C_xH_{2y+1}^+$ are exothermic, except for two of the chain structures of $C_5H_9^+$, which hence is believed not to contribute significantly to the $C_5H_9^+$ population. Based on the general reactivity pattern of ions involved in charge transfer and hydride transfer just described, that the observed reactions are exothermic and vice versa, the lack of the hydride transfer of $C_3H_3^+$ or $C_5H_7^+$ can be considered as an indication that only the cyclic structure is present in these ions' population because otherwise the chain structures would make the hydride transfer exothermic. $C_4H_5^+$ also lacks the hydride transfer, suggesting methylcyclopropenylium as the only isomer present. Please note, however, that the ion population refers to the one after a 500-ms cooling period (see Section 2), during which some highly reactive species may have been reacted away. This notion applies to similar discussion elsewhere in this paper.

For those reactive even-electron ions, there is a general trend in their reaction efficiency (ratio of $k_{exp.}/k_{coll.}$) that it decreases as the mass of the reactant ion increases, except for $C_6H_{11}^+$.

### 4.4. Reactions of odd-electron ions

$C_7H_{13}^+$ is also a major product ion in odd-electron ion reactions, and is formed via hydride transfer mechanism by similar arguments as for the even-electron ions, that is, the results of the isotope distribution and the exothermicity constraints. In the reaction of $C_2H_4^{+\bullet}$ or $C_3H_6^{+\bullet}$, the ion $C_7H_{14}^{+\bullet}$ is also produced, via charge transfer, as suggested by the isotope distribution when deuterated reagents are used:

$$C_2D_4^{+\bullet} + C_7H_{14} \rightarrow C_7H_{14}^{+\bullet} + C_2D_4 \quad (3)$$

$$C_3D_6^{+\bullet} + C_7H_{14} \rightarrow C_7H_{14}^{+\bullet} + C_3D_6. \quad (4)$$

The relationship between the reactivities of the charge transfer and hydride transfer with enthalpies of reaction is also apparent from Table 4: the observed reactions are exothermic and vice versa, consistent with earlier findings [42], with a few exceptions for certain structural isomers. For $C_4H_8^+$ there appear to be no cyclic isomers, since the cyclic isomers would make the charge transfer exothermic, which is not observed. Similarly, isomer $CH{\equiv}CCH_2CH_3^{+\bullet}$ for

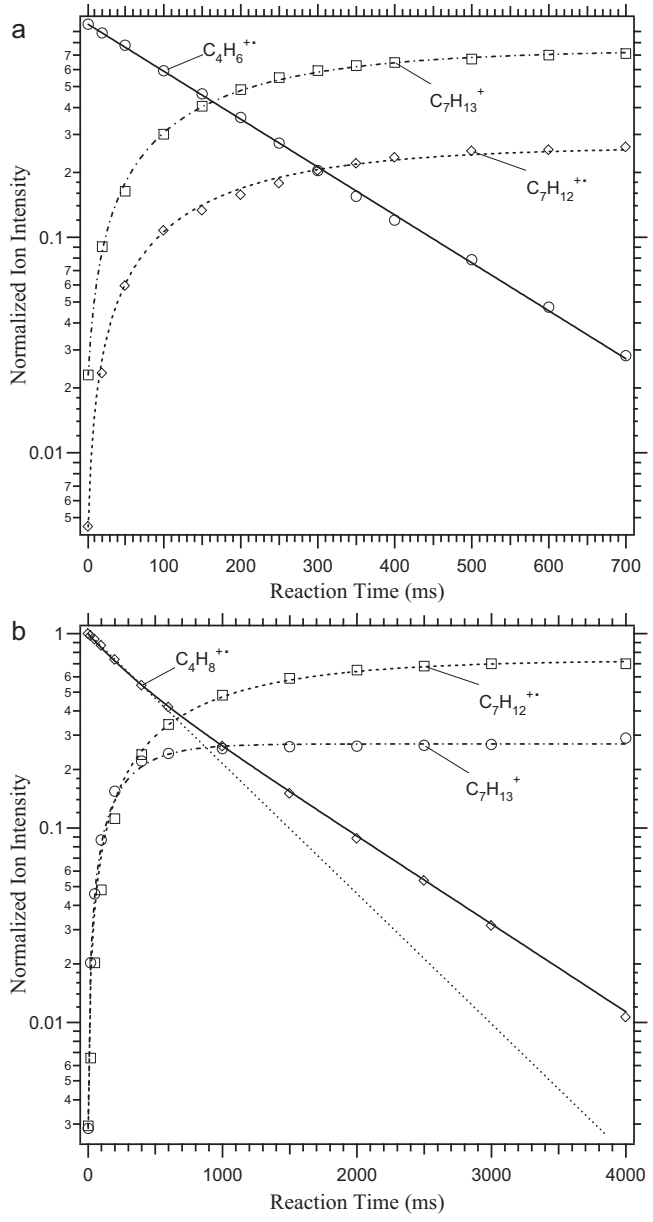


**Fig. 3.** Reaction time dependencies of ion intensities in the reaction of (a) $C_4H_6^{+\bullet}$ and (b) $C_4H_8^{+\bullet}$ with MCH. Symbols are experimental data, while dashed lines are the fits of kinetic models described in the text. The dotted tangent line for $C_4H_8^+$ data represents the initial decay rate of this ion.

$C_4H_6^{+\bullet}$, isomers $C_3H_7C{\equiv}CH^{+\bullet}$ and $(CH_3)_2CHC{\equiv}CH^{+\bullet}$ for $C_5H_8^{+\bullet}$, and methylcyclobutane radical cation for $C_5H_{10}^{+\bullet}$ are considered to be absent from the population of these ions.

All odd-electron ions except $C_2H_4^{+\bullet}$ produce a significant amount of $C_7H_{12}^{+\bullet}$, most likely via $H_2^{-\bullet}$ transfer mechanism:

$$B^{+\bullet} + C_7H_{14} \rightarrow C_7H_{12}^{+\bullet} + BH_2. (B^{+\bullet}: \text{odd-electron ions}) \quad (5)$$

When the deuterated reactant ions are used, the product ions show no retention of D atom from the reactant ions, as shown below for the reactions of $C_4H_6^{+\bullet}$ as an example:

$$C_4D_6^{+\bullet} + C_7H_{14} \rightarrow C_7H_{12}^{+\bullet} + C_4D_6H_2.$$

The enthalpies of reactions listed in Table 4 for the formation of $C_7H_{12}^{+\bullet}$ are based on the assumption of $H_2^{-\bullet}$ transfer mechanism (5).

For the odd-electron ions there is also a similar trend in the reaction efficiency ($k_{exp.}/k_{coll.}$) as for the even-electron ions: in general it decreases with the increasing masses of reactant ions, as expected from trends in ionization energy [43].

Below are additional discussions on some individual odd-electron ion reactions.

#### 4.4.1. Reaction of $C_2H_4^{+\bullet}$

It is interesting to note the lack of $H_2^{-\bullet}$ transfer for $C_2H_4^{+\bullet}$ although it is exothermic by 202 kJ/mol. In addition to the charge transfer and hydride transfer products, the $C_2H_4^{+\bullet}$ reaction with MCH produces $C_6H_{11}^+$, presumably by methide ($CH_3^-$) transfer, with the isotope distribution when using isotope reagents as:

$$C_2D_4^{+\bullet} + C_7H_{14} \rightarrow C_6H_{11}^+ + C_3D_4H_3^\bullet \quad (6)$$

This reaction is exothermic by 77.8 kJ/mol (Table 4). Other possible mechanisms include dissociative charge transfer (7) and dissociative hydride transfer (8):

$$C_2H_4^{+\bullet} + C_7H_{14} \rightarrow C_6H_{11}^+ + CH_3^\bullet + C_2H_4 \quad (7)$$

$$C_2H_4^{+\bullet} + C_7H_{14} \rightarrow C_6H_{11}^+ + CH_2 + C_2H_5^\bullet, \quad (8)$$

but they are endothermic by 19.7 and 329.7 kJ/mol, respectively, calculated using published thermochemical data from Ref. [55].

#### 4.4.2. Reaction of $C_3H_6^{+\bullet}$

Beside the products of charge transfer, hydride transfer and $H_2^{-\bullet}$ transfer, the reaction of $C_3H_6^{+\bullet}$ also produces $C_6H_9^+$. The result with isotope reagents is:

$$C_3D_6^{+\bullet} + C_7H_{14} \rightarrow C_6H_9^+ + \text{neutral products.} \quad (9)$$

The two most likely mechanisms are dissociative hydride transfer (10) and dissociative $H_2^{-\bullet}$ transfer (11):

$$C_3H_6^{+\bullet} + C_7H_{14} \rightarrow C_6H_9^+ + CH_4 + C_3H_7^\bullet \quad (10)$$

$$C_3H_6^{+\bullet} + C_7H_{14} \rightarrow C_6H_9^+ + CH_3^\bullet + C_3H_8 \quad (11)$$

If the reactant ion $C_3H_6^{+\bullet}$ is a linear structure as shown by (i) in Table 4, the enthalpies of reaction are 14.5 kJ/mol and 37 kJ/mol for (10) and (11), respectively. And if $C_3H_6^{+\bullet}$ is a cyclic structure (ii), they are −23.3 kJ/mol and −8 kJ/mol, respectively. Another possible mechanism, dissociative charge transfer, is endothermic, no matter whether neutral products are $CH_4 + H^\bullet + C_3H_6$ or $CH_3^\bullet + H_2 + C_3H_6$, and whether the reactant ion $C_3H_6^{+\bullet}$ is a linear or cyclic structure. In summary, we believe that the cyclic isomer of $C_3H_6^{+\bullet}$ is responsible for the formation of $C_6H_9^+$, via hydride transfer or $H_2^{-\bullet}$ transfer. The experimental data of the time dependencies of ion intensities show signs of the existence of more than one isomer of $C_3H_6^{+\bullet}$ with different reactivities, as mentioned earlier. The kinetic data presented in Table 4 (branching ratios and rate constants) are derived from the fitting of the experimental data using the following two-isomer reaction model:

$$C_3H_6^{+\bullet}(\text{i}) + C_7H_{14} \rightarrow C_7H_{13}^+ + C_3H_7^\bullet (69\%) \quad (12)$$

$$C_3H_6^{+\bullet}(\text{i}) + C_7H_{14} \rightarrow C_7H_{12}^{+\bullet} + C_3H_8 (31\%) \quad (13)$$

$$C_3H_6^{+\bullet}(\text{ii}) + C_7H_{14} \rightarrow C_7H_{14}^{+\bullet} + C_3H_6 (46\%) \quad (14)$$

$$C_3H_6^{+\bullet}(\text{ii}) + C_7H_{14} \rightarrow C_7H_{13}^+ + C_3H_7^\bullet (38\%) \quad (15)$$

$$C_3H_6^{+\bullet}(\text{ii}) + C_7H_{14} \rightarrow C_6H_9^+ + (CH_4 + C_3H_7^\bullet \text{ or } CH_3^\bullet + C_3H_8) (16\%) \quad (16)$$

where $C_3H_6^{+\bullet}$ (i) represents the linear isomer $[CH_3CH{=}CH_2]^{+\bullet}$, and $C_3H_6^{+\bullet}$ (ii), the cyclic isomer $[c\text{-}C_3H_6]^{+\bullet}$. The branching ratios of different reaction channels for each isomer, derived from the data fittings, are shown in parentheses. The data fitting also gives the

percent populations of the linear and cyclic isomers as 74% and 26%, respectively.

#### 4.4.3. Reaction of $C_4H_8^{+\bullet}$

Only a negligible amount of the charge transfer product ion $C_7H_{14}^{+\bullet}$ is observed, suggesting an insignificant contribution to the $C_4H_8^{+\bullet}$ population from the cyclic structure that could have an exothermic charge transfer by 26.9 kJ/mol. As seen from Fig. 3b and discussed earlier, multiple isomers exist in the $C_4H_8^{+\bullet}$ population that react with MCH differently. The kinetic data shown in Table 4 is derived from the data fitting based on the following reaction model:

$$C_4H_8^{+\bullet}(\text{i}) + C_7H_{14} \rightarrow C_7H_{12}^{+\bullet} + C_4H_{10}(< 0.1\%) \quad (17)$$

$$C_4H_8^{+\bullet}(\text{i}) + C_7H_{14} \rightarrow C_7H_{13}^{+} + C_4H_9^{\bullet}(100\%) \quad (18)$$

$$C_4H_8^{+\bullet}(\text{ii}) + C_7H_{14} \rightarrow C_7H_{12}^{+\bullet} + C_4H_{10}(100\%). \quad (19)$$

$C_4H_8^{+\bullet}$ (i) represents either or both isomers $[CH_3CH_2CH{=}CH_2]^{+\bullet}$ and $[(CH_3)_2C{=}CH_2]^{+\bullet}$, while $C_4H_8^{+\bullet}$ (ii), isomers [(Z)-$CH_3CH{=}CHCH_3]^{+\bullet}$ and [(E)-$CH_3CH{=}CHCH_3]^{+\bullet}$. The hydride transfer for isomers [(Z)-$CH_3CH{=}CHCH_3]^{+\bullet}$ and [(E)-$CH_3CH{=}CHCH_3]^{+\bullet}$ is endothermic and therefore is not included in the above reaction model. It is interesting to note that although the $H_2^{-\bullet}$ transfer for isomers $[CH_3CH_2CH{=}CH_2]^{+\bullet}$ and $[(CH_3)_2C{=}CH_2]^{+\bullet}$ is exothermic, its branching ratio derived from the data fitting is negligibly small. The data fitting results in the percentage of isomers $C_4H_8^{+\bullet}$ (i) and $C_4H_8^{+\bullet}$ (ii) as 27% and 73%, respectively.

#### 4.4.4. Reaction of $C_5H_{10}^{+\bullet}$

$C_5H_{10}^{+\bullet}$ undergoes no charge or hydride transfer but does exhibit $H_2^{-\bullet}$ transfer with MCH. Based on these reactivities and the thermochemical data in Table 4, it is proposed that only isomers $[Z\text{-}CH_3CH_2CH{=}CHCH_3]^{+\bullet}$, $[E\text{-}CH_3CH_2CH{=}CHCH_3]^{+\bullet}$ and/or $[(CH_3)_2CHCH{=}CH_2]^{+\bullet}$ compose the majority of the $C_5H_{10}^{+\bullet}$ population. In the study by Gaumann et al., [56] it was found that the collisional dissociation of the parent ion, $C_7H_{14}^{+\bullet}$, produces $C_5H_{10}^{+\bullet}$ through two major channels: by the loss of ethylene from the 2,3 position (60%), and by the loss of ethylene from the 3,4 position (30%), which most likely results in products $[CH_3CH_2CH{=}CHCH_3]^{+\bullet}$ and $[(CH_3)_2CHCH{=}CH_2]^{+\bullet}$, respectively.

## 5. Summary

Electron ionization of $C_7H_{14}$ generates the parent ion $C_7H_{14}^{+\bullet}$ and fragment ions $C_6H_{11}^{+}$ and $C_4H_7^{+}$ as the most important product ions, with the total cross section reaching a soft maximum of $17.7 \times 10^{-16}$ cm$^2$ at ~65 eV. Other significant product ions at low energies (<30 eV) include $C_6H_{10}^{+\bullet}$, $C_5H_{10}^{+\bullet}$, $C_5H_9^{+}$, $C_4H_8^{+\bullet}$, $C_3H_6^{+\bullet}$ and $C_3H_5^{+}$.

Ab initio BEB calculations predict that the total cross section reaches a maximum of $21.0 \times 10^{-16}$ cm$^2$ at 70 eV. This is in reasonable agreement with the experimental measurement. In general, the experimental data are smaller than the theoretical ones at most of the electron energies, probably indicating that the production of $H^+$, which our current FTMS method cannot detect, is significant in the electron ionization of $C_7H_{14}$, or a certain amount of fragment ions is produced with kinetic energies greater than the limit in which our current FTMS method can trap the ions. Further investigation on these issues is underway.

The subsequent ion-molecule reactions between $C_7H_{14}$ and selected fragment ions are studied. All even-electron ions ($C_xH_{2y+1}^{+}$) undergo only hydride transfer, except $C_3H_3^{+}$, $C_4H_5^{+}$ and $C_5H_7^{+}$ which are unreactive. All odd-electron ions ($C_xH_{2y}^{+\bullet}$) except $C_5H_8^{+\bullet}$, $C_5H_{10}^{+\bullet}$ and $C_6H_{10}^{+\bullet}$ also undergo hydride transfer as a major reaction channel, with charge transfer and $H_2^{-\bullet}$ transfer as additional channels for some of the odd-electron ions. The reaction of $C_2H_4^{+\bullet}$ also forms $C_6H_{11}^{+}$ by methide transfer, and reaction of $C_3H_6^{+\bullet}$ also forms $C_6H_9^{+}$ by dissociative hydride transfer or $H_2^{-\bullet}$ transfer. With a few exceptions, the reactivities can be explained by thermochemical data, i.e., the observed reactions are exothermic and vice versa. For those reactive ions, the reaction rate constants range from $0.083 \times 10^{-10}$ to $16 \times 10^{-10}$ cm$^3$/s, and there is a trend in the reaction efficiency that it decreases as a function of the increasing mass of the reactant ion.

Based on their reactivities, it is proposed that $C_3H_3^{+}$ and $C_5H_7^{+}$ have only cyclic structures, while $C_4H_8^{+\bullet}$ and $C_5H_{10}^{+\bullet}$, on the other hand, have no cyclic structures. $C_3H_6^{+\bullet}$ and $C_4H_8^{+\bullet}$ are each found to be a mixture of different isomers having different reactivities toward $C_7H_{14}$, while other ions may be composed by only one isomer or possibly several isomers with similar reactivities. The above discussion of the ion composition refers to the ion population after 500 ms from the electron ionization, during which ions are thermalized and some of the highly reactive isomers may have been reacted away.

## Acknowledgements

The authors thank the Propulsion Directorate AFRL, the Air Force Office of Scientific Research and NIST for their support.

## References

[1] A. Violi, S. Yan, E.G. Eddings, A.F. Sarofim, S. Granata, T. Faravelli, E. Ranzi, Combust. Sci. Technol. 174 (2002) 399.
[2] J. Yu, S. Eser, Ind. Eng. Chem. Res. 34 (1995) 404.
[3] C.K. Westbrook, Proc. Combust. Inst. 28 (2000) 1563.
[4] A. Agosta, N.P. Cernansky, D.L. Miller, T. Faravelli, E. Ranzi, Exp. Therm. Fluid Sci. 28 (2004) 701.
[5] J.A. Cooke, M. Belluci, M.D. Smooke, A. Gomez, A. Violi, T. Faravelli, E. Ranzi, Proc. Combust. Inst. 30 (2005) 439.
[6] S. Humer, A. Frassoldati, S. Granata, T. Faravelli, E. Ranzi, R. Seiser, K. Seshadri, Proc. Combust. Inst. 31 (2007) 393.
[7] W.J. Pitz, C.V. Naik, T. Mhaolduin Ni, C.K. Westbrook, H.J. Curran, J.P. Orme, J.M. Simmie, Proc. Combust. Inst. 31 (2007) 267.
[8] S. Zeppieri, K. Brezinsky, I. Glassman, Combust. Flame 108 (1997) 266.
[9] J.P. Orme, H.J. Curran, J.M. Simmie, J. Phys. Chem. A 110 (2006) 114.
[10] Y. Yang, J.P. Szybist, A.L. Boehman, Prepr. Pap.-Am. Chem. Soc., Div. Fuel Chem. 51 (2006) 329.
[11] Y. Yang, J.V. Zello, A.L. Boehman, Prepr. Pap.-Am. Chem. Soc., Div. Fuel Chem. 52 (2007) 753.
[12] S.S. Vasu, D.F. Davidson, R.K. Hanson, Combust. Flame 156 (2009) 736.
[13] A.J. Midey, S. Williams, T.M. Miller, A.A. Viggiano, Int. J. Mass Spectrom 222 (2003) 413.
[14] S. Williams, A.J. Midey, S.T. Arnold, T.M. Miller, P.M. Bench, R.A. Dressler, Y.H. Chiu, D.J. Levandier, A.A. Viggiano, R.A. Morris, M.R. Berman, L.Q. Maurice, C.D. Carter, AIAA Fourth Weakly Ionized Gases Workshop, Anaheim, CA, 2001.
[15] D.B. Milligan, P.F. Wilson, C.G. Freeman, M. Meot-Ner, M.F. McEwan, J. Phys. Chem. A 106 (2002) 9745.
[16] P. Spanel, M. Pavlik, D. Smith, Int. J. Mass Spectrom. Ion Process. 145 (1995) 177.
[17] L.W. Sieck, M. Mautner (Meot-Ner), J. Phys. Chem. 86 (1982) 3646.
[18] Y.-K. Kim, M.E. Rudd, Phys. Rev. A 50 (1994) 3954–3967.
[19] W. Hwang, Y.-K. Kim, M.E. Rudd, J. Chem. Phys. 104 (1996) 2956–2966.
[20] Certain commercial materials and equipment are identified in this paper in order to specify procedures completely. In no case does such identification imply recommendation or endorsement by the National Institute of Standards and Technology, the United States Air Force, or UES Inc., nor does it imply that the material or equipment identified is necessarily the best available for the purpose.
[21] C.Q. Jiao, C.A. DeJoseph Jr., A. Garscadden, J. Vac. Sci. Technol. A 23 (2005) 1295.
[22] C.Q. Jiao, C.A. DeJoseph Jr., R. Lee, A. Garscadden, Int. J. Mass Spectrom. 257 (2006) 34.
[23] M.B. Comisarow, A.G. Marshall, Chem. Phys. Lett. 25 (1974) 282.
[24] A.G. Marshall, P.B. Grosshans, Anal. Chem. 63 (1991) 215A.
[25] Z. Liang, A.G. Marshall, Anal. Chem. 62 (1990) 70.
[26] A.G. Marshall, T.L. Wang, T.L. Ricca, J. Am. Chem. Soc. 107 (1985) 7983.
[27] S. Guan, Chem. Phys. 91 (1989) 775.
[28] L. Chen, A.G. Marshall, Int. J. Mass Spectrom. Ion Processes 79 (1987) 115.
[29] H.C. Straub, P. Renault, B.G. Lindsay, K.A. Smith, R.F. Stebbings, Phys. Rev. A 52 (1995) 1115.

[30] Y.-K. Kim, K.K. Irikura, M.E. Rudd, M.A. Ali, P.M. Stone, J. Chang, J.S. Coursey, R.A. Dragoset, A.R. Kishore, K.J. Olsen, A.M. Sansonetti, G.G. Wiersma, D.S. Zucker, M.A. Zucker, Electron-Impact Cross Sections for Ionization and Excitation Database, version 3.0, National Institute of Standards and Technology, Gaithersburg, MD, 2005, http://physics.nist.gov/ionxsec.
[31] I. Torres, R. Martínez, M.N. Sánchez Rayo, F. Castaño, J. Chem. Phys 115 (2001) 4041–4050.
[32] S. Popović, S. Williams, L. Vušković, Phys. Rev. A 73 (2006) 022711.
[33] A.D. Becke, J. Chem. Phys. 98 (1993) 5648–5652.
[34] P.J. Stephens, F.J. Devlin, C.F. Chabalowski, M.J. Frisch, J. Phys. Chem. 98 (1994) 11623–11627.
[35] W. von Niessen, J. Schirmer, L.S. Cederbaum, Comput. Phys. Rep. 1 (1984) 57–125.
[36] V.G. Zakrzewski, J.V. Ortiz, J. Phys. Chem. 100 (1996) 13979–13984.
[37] K. Raghavachari, G.W. Trucks, J.A. Pople, M. Head-Gordon, Chem. Phys. Lett. 157 (1989) 479–483.
[38] T.H. Dunning Jr, J. Chem. Phys. 90 (1989) 1007–1023.
[39] K. Watanabe, T. Nakayama, J. Mottl, J. Quant. Spectrosc. Rad. Transf. 2 (1962) 369–382.
[40] S. Rang, P. Poldoia, A. Talvari, Eesti NSV Tead. Akad. Toim. 23 (1974) 354–357.
[41] M. Meot-ner (Mautner), L.W. Sieck, P.J. Ausloos, Am. Chem. Soc. 103 (1981) 5342–5348.
[42] L.W. Sieck, M. Mautner (Meot-Ner), J. Phys. Chem. 86 (1982) 3646–3650.
[43] J.L. Holmes, F.P. Lossing, Org. Mass Spectrom. 26 (1991) 537–541.
[44] K.K. Irikura, R.D. Johnson III, R.N. Kacker, R. Kessel, J. Chem. Phys. 130 (2009) 114102.
[45] M.J. Frisch, G.W. Trucks, H.B. Schlegel, G.E. Scuseria, M.A. Robb, J.R. Cheeseman, J.A. Montgomery Jr., T. Vreven, K.N. Kudin, J.C. Burant, J.M. Millam, S.S. Iyengar, J. Tomasi, V. Barone, B. Mennucci, M. Cossi, G. Scalmani, N. Rega, G.A. Petersson, H. Nakatsuji, M. Hada, M. Ehara, K. Toyota, R. Fukuda, J. Hasegawa, M. Ishida, T. Nakajima, Y. Honda, O. Kitao, H. Nakai, M. Klene, X. Li, J.E. Knox, H.P. Hratchian, J.B. Cross, V. Bakken, C. Adamo, J. Jaramillo, R. Gomperts, R.E. Stratmann, O. Yazyev, A.J. Austin, R. Cammi, C. Pomelli, J.W. Ochterski, P.Y. Ayala, K. Morokuma, G.A. Voth, P. Salvador, J.J. Dannenberg, V.G. Zakrzewski, S. Dapprich, A.D. Daniels, M.C. Strain, O. Farkas, D.K. Malick, A.D. Rabuck, K. Raghavachari, J.B. Foresman, J.V. Ortiz, Q. Cui, A.G. Baboul, S. Clifford, J. Cioslowski, B.B. Stefanov, G. Liu, A. Liashenko, P. Piskorz, I. Komaromi, R.L. Martin, D.J. Fox, T. Keith, M.A. Al-Laham, C.Y. Peng, A. Nanayakkara, M. Challacombe, P.M.W. Gill, B. Johnson, W. Chen, M.W. Wong, C. Gonzalez, Pople, J. A. Gaussian 03, revision E. 01, Gaussian, Inc., Wallingford, CT, 2004.
[46] A. Streitwieser Jr., C.H. Heathcock, Introduction to Organic Chemistry, Macmillan, New York, 1976.
[47] L.A. Curtiss, P.C. Redfern, K. Raghavachari, V. Rassolov, J.A. Pople, J. Chem. Phys. 110 (1999) 4703–4709.
[48] D.H. Williams, I. Howe, Principles of Organic Mass Spectrometry, McGraw-Hill, London, 1972.
[49] N. Durić, I. Čadež, M. Kurepa, Int. J. Mass Spectrom. Ion Proc. 108 (1991) R1–R10.
[50] H. Nishimura, H.J. Tawara, Phys. B-At. Mol. Opt. Phys. 27 (1994) 2063–2074.
[51] B.L. Schram, M.J. van der Wiel, F.J. de Heer, H.R. Moustafa, J. Chem. Phys. 44 (1966) 49–54.
[52] P. Wang, C.R. Vidal, J. Chem. Phys. 116 (2002) 4023.
[53] D.R. Lide (Ed.), CRC Handbook of Chemistry and Physics, 81st ed., CRC Press, Boca Raton, FL, 2000.
[54] R. Houriet, G. Parisod, T. Gaumann, J. Am. Chem. Soc. 99 (1977) 3599.
[55] S.G. Lias, J.E. Bartmess, J.F. Liebman, J.L. Holmes, R.D. Levin, W.G. Mallard, Gas-phase ion neutral thermochemistry, J. Phys. Chem. Ref. Data 17 (1988).
[56] T. Gaumann, A. Heusler, S. Haebel, W. Feng, Eur. Mass Spectrom 4 (1998) 333.
[57] M. Rosenstock, K. Draxl, B.W. Steiner, J.T. Herron, Energetics of gaseous ions, J. Phys. Chem. Ref. Data 6 (1977).